The molecular origin of birefringence in skeletal muscle

Contribution of myosin subfragment S-1

H. Martin Jones,* R. J. Baskin,*§ and Y. Yeh‡§

*Departments of Zoology and ‡Applied Science and the §Graduate Group in Biophysics, University of California, Davis, California

ABSTRACT The state of optical polarization of He-Ne laser light diffracted by single skinned frog skeletal muscle fibers has been determined after decoration of the thin filaments of rigor fibers with exogenous S-1. Light on the first diffraction order was analyzed using optical ellipsometry for changes occurring in total birefringence (Δn_T) and total differential field ratio (r_T) and the experimental results compared with theoretical predictions. Fibers were examined with SDS-gel electrophoresis and electron microscopy as independent assays of S-1 binding. The binding of S-1 to the thin filaments caused a significant increase in r_T and a small but significant decrease in Δn_T. Release of bound exogenous S-1 with magnesium pyrophosphate demonstrated that the effect of S-1 on the optical parameters was reversible and both electrophoresis and electron microscopy demonstrated the presence of S-1 specifically bound to the thin filaments. Model simulations based on the theory of Yeh, Y., and R. Baskin (1988. *Biophys. J.* 54:205–218) showed that the values of Δn_T and r_T were sensitive to the axial bonding angle of exogenous S-1 as well as to the volume fraction of added S-1. Analysis of the data in light of the model showed that an average axial S-1 binding angle of 68° ± 7° best fit the data.

INTRODUCTION

The orderly arrangement of repeating structural units in skeletal muscle, the sarcomere, and its molecular components, have enabled researchers to use methods adopted from crystallography, e.g., x-ray and laser diffraction, optical averaging techniques, and polarized light analysis, to pinpoint the structural relationships of many of the proteins involved in the functioning of the muscle. Current evidence points conclusively to the myosin cross-bridge having a structurally dynamic character and playing a dominant role in the production of tension in skeletal muscle. Even though the cross-bridge theory of muscle contraction is almost universally accepted, the role and action of the cross-bridge are still widely and vigorously debated. The monitoring of birefringence changes is potentially one of the most valuable tools in determining the orientation of cross-bridges that accompany the various physiological and experimental states of a muscle fiber; it is noninvasive and sensitive to changes in dimension and orientation on the macromolecular level. Many studies have monitored the birefringence changes of muscle under conditions that are thought to produce changes in cross-bridge orientation (Irving and Peckham, 1986; Peckham and Irving, 1989; Taylor, 1975, 1976). The interpretation of the source of the signal has been complicated by the two related yet distinct types of anisotropy, form and intrinsic, that interact to produce the total birefringence of skeletal muscle. The evaluation of polarized light passing through a muscle fiber has recently been advanced by the technique of optical ellipsometry conducted on the diffraction order (Baskin et al., 1986), and it is the subject of this paper to investigate the effect on the optical signal of myosin subfragment-1 decoration of thin filaments in isolated, skinned fibers. The experimental data will be analyzed using a model system based on our theoretical development (Yeh and Baskin, 1988; Chen et al., 1989). In this model we are able to show the relationship between the experimental results and predictions of the exogenous S-1 axial binding angle. We will show that the data is consistent with an average angle of 68° ± 7°.

Studies of the transmission birefringence of muscle fibers have reduced the form component to a minimum by index matching. This procedure typically replaces the aqueous medium bathing the fiber with a succession of solvents having increasing indices of refraction. When the medium's index of refraction approaches that of protein the form elements no longer contribute to the Δn_T; the form component has thus been matched out and the residual, or remaining birefringence, is an approximation of the intrinsic component (e.g., Colby, 1971). Due to the denaturing effects of the combined treatments with fixatives and organic solvents, the structure, and therefore the optical properties of the muscle, are altered. Therefore, this procedure results in information not easily applicable to the native or unfixed state. We note, however, a report by Obiorah and Irving

Address correspondence to Dr. Baskin.

0006-3495/91/11/1217/12 $2.00

(1989) in which they argue that the intrinsic birefringence of rigor rabbit psoas muscle fibers was not detectably altered by glutaraldehyde fixation, dehydration in dimethyl sulfoxide, and immersion in nonaqueous imbibing media. Their conclusion was based on the similarity between data obtained using the above procedure and one in which the form birefringence was matched out in aqueous media (61% by weight metrizamide). Their reported value for intrinsic birefringence, $\sim 1 \times 10^{-3}$, generally agrees with previously published results (Colby, 1971; Taylor, 1976).

We demonstrate in this investigation that the differential field ratio (DFR) is a consistently sensitive probe of both the presence and average angle of orientation of exogenous S-1 decorating the thin filaments. From the combined data of DFR and birefringence, we derive the average axial binding angle for the S-1 attachment by comparing theoretical models with data obtained from skinned single frog muscle fibers that were decorated with exogenous S-1. This approach avoids the need to index match the muscle proteins.

MATERIALS AND METHODS

Preparation of single skinned muscle fibers

All procedures were carried out at 4–6°C unless stated otherwise.

Single intact muscle fibers were dissected from the lateral head of the anterior tibialis muscle of grass frogs (*Rana sp.*) bathed in chilled amphibian Ringer's solution, mounted on small coverslips by means of aluminum clips attached directly to the tendonous insertions of the fiber, soaked for 30 min in relaxing solution (75 mM K^+ acetate, 5 mM Mg^{2+} acetate, 5 mM EGTA, 15 mM phosphate buffer, pH 7.1, and 5 mM ATP [Magid and Reedy, 1980]), chemically skinned for 15 min in relaxing solution plus 0.5% Triton X-100, 0.4 mM PMSF, 1 μg/ml leupeptin, 30 μg/ml pepstatin, 75 μg/ml *N*-tosyl-L-phenylalanine chloromethyl ketone (TPCK), and 10 μg/ml Nα-*p*-tosyl-L-lysine chloromethyl ketone (TLCK), and finally returned to fresh relaxing solution. Fibers not used that day were incubated overnight in relaxing solution/50% glycerol plus 0.025% (wt/vol) sodium azide and subsequently stored for periods of up to 2 mo at −20°C. The stored fibers were rinsed with three changes of relaxing solution for a minimum of 1 h before use in optical experiments.

Preparation of proteins

All of the exogenous proteins were prepared from adult male New Zealand white rabbits. (The animals were euthanized with an overdose of barbiturate and the psoas, back, and leg muscles removed and placed on ice for 1 h. Myosin was prepared from this material [Margossian and Lowey, 1982] or from glycerinated myofibrils [Thomas et al., 1980]. Ion exchange purification of the myosin-enriched fraction was performed on a 2.5 × 50-cm column of DEAE cellulose (Whatman Inc. DE-52; Clifton, NJ) using a linear gradient of 30 mM sodium pyrophosphate, 1 mM DTT to 0.5 M sodium chloride in 30 mM sodium pyrophosphate, 1 mM DTT. Purified myosin was dialyzed vs. 50% glycerol, 0.5 M NaCl, 5 mM TES, 0.5 mM DTT, 0.5 mM EDTA, pH 7.1, and stored at −20°C).

S-1 was prepared from glycerinated myofibrils by a modification of a procedure described by Thomas et al. (1980). Glycerinated myofibrils were diluted 1:1 with 100 mM KCl, 10 mM imidazole, and 3 mM EDTA, pH 7.2, and centrifuged for 10 min at 2,250 rpm using a Sorvall GSA rotor (DuPont Co., Wilmington, DE). The supernatant was discarded and the pelleted myofibrils washed twice more with fresh buffer. The myofibrils were digested at room temperature for 20 min with TLCK-alpha-chymotrypsin at an enzyme/myosin ratio of 1:150. The digestion was stopped by the addition of PMSF to a concentration of 1 mM and the mixture centrifuged for 20 min at 10,000 rpm in a GSA rotor. The myofibrils were washed twice with 100 mM KCl, 5 mM EGTA, 10 mM $MgCl_2$, 10 mM imidazole, pH 7.1, and ATP added to a final concentration of 5 mM. The mixture was stirred on ice for 10 min, DTT added to a concentration of 1 mM and centrifuged for 35 min at 10,000 rpm in a GSA rotor. The supernatant was saved and fractionated with saturated ammonium sulfate (neutralized and containing 10 mM EDTA). The fraction precipitating between 37 and 70% was pelleted by centrifuging for 90 min at 12,000 rpm in a GSA rotor. The pellets were resuspended in a minimum volume of 50 mM imidazole, 1 mM DTT, and 0.025% sodium azide, pH 7.1, and dialyzed exhaustively against this buffer overnight. The dialysate was clarified by centrifuging for 30 min at 16,000 rpm in an SS34 rotor. Anion exchange chromatography was performed using a 2.5 × 10-cm column of DEAE-Sephacel equilibrated in 50 mM imidazole, 1 mM DTT, pH 7.1. The sample was applied in 2.5 column volumes and the column eluted with a gradient of 0 to 150 mM NaCl in the column buffer. Major peak fractions were examined by SDS-PAGE and those containing only S-1 were pooled, concentrated using nitrogen-pressurized ultrafiltration (Amicon Corp. [Danvers, MA] model 8050 with a YY30 membrane) in the cold room, and lyophilized in elution buffer plus 10% sucrose and 0.025% sodium azide.

Approximately 8–10 mg of lyophilized material was reconstituted in incubation buffer (mM): 75 K^+ acetate, 5 Mg^{2+} acetate, 1 DTT, 5 EGTA, 15 K^+ phosphate, pH 7.1, to a total volume of 3 ml, and then passed through a buffer exchange column (Bio-gel P10 gel desalting column from Bio-Rad, Inc., Richmond, CA) equilibrated in the same buffer. This material was used for optical studies on the day of reconstitution.

General experimental design

The approach taken here was to alter the volume fraction of specific regions of the sarcomeres of skinned muscle fibers by decorating the thin filaments with S-1. The purpose of these experiments was to measure the steady-state change due to the binding of S-1 to the thin filaments. A muscle fiber was placed into rigor at a given sarcomere length and S-1 added to the medium to a final concentration of ~1 mg/ml. The duration of the S-1 incubation step typically continued until the first order diffraction intensity had declined to at least 50% of its original value. This interval varied and depended on such factors as sarcomere length (sl), fiber diameter, and S-1 concentration. The first order diffraction intensity is an indicator of the relative A-band/I-band refractive index differential, i.e., the relative difference in mass density. As the differential become less, in this case due to S-1 binding to the thin filaments, there would be a decrease in the first order diffraction intensity. After incubation the medium was replaced with fresh rigor medium without S-1, optical data collected, and the fiber processed immediately for SDS-PAGE or the experiment continued. The continuation involved further S-1 incubation or a MgPPi treatment to release S-1. A few fibers were processed for electron microscopy at various steps instead of SDS-PAGE. The solutions that were used during optical measurements all had an ionic strength of ~100 mM, a value known to result in no appreciable change in lattice spacing upon change of fiber state (Matsubara and Elliott, 1972; Brenner et al., 1984).

Optical studies

The optical studies were designed to measure the optical parameters phase angle (δ, the shift in degrees between the orthogonal components) and the differential ellipticity (or field) ratio:

$$r_T = \frac{\sqrt{I_{II}}/\text{Cos}\ \theta_D - \sqrt{I_\perp}}{\sqrt{I_{II}}/\text{Cos}\ \theta_D + \sqrt{I_\perp}}$$

where θ_D is the diffraction angle of a steady-state interval during the incubation of a muscle fiber with S-1. The parameter I is the amplitude of the respective parallel or perpendicular orthogonal component of the intensity. Knowledge of these parameters permits the complete description of the state of polarization of light that has interacted with a muscle fiber. Birefringence, Δn_T, was computed from the phase angle and fiber diameter according to the following:

$$\Delta n_T = \delta(\lambda/360)/d,$$

where d is the fiber diameter, λ is the wavelength of light used (0.6328 μm), and 360 converts radians to degrees. The muscle fiber was placed into a temperature-controlled chamber filled with relaxing solution (incubation buffer plus 4 mM ATP) and the sl and fiber-axis orientation adjusted. Linearly polarized He-Ne laser light with its axis of transmission normal to, and its plane of polarization at 45° to, the fiber longitudinal axis was diffracted by the muscle fiber into well defined orders. The light at the first order was analyzed with a quarter-wave plate ellipsometer during steady-state intervals of the incubation. The ellipsometer consists of two optically aligned components: a quarter-wave plate whose fast axis rotates through 180°, followed by a Glan-Taylor prism whose axis is fixed at zero degrees. A light pipe permits the intensity of light transmitted by the ellipsometer to be fed to a photomultiplier tube which is interfaced with a computer. The quarter-wave plate is rotated by a computer-controlled stepping motor and the intensity variation due to this rotation is stored as a function of the angle of rotation of the fast axis of the quarter-wave plate. The diameter of each fiber, in each solution, was measured microscopically using a filar eyepiece. The accuracy of this measurement was 3–5%.

Gel electrophoresis

In each case it was ascertained with electrophoresis (Laemmli, 1970) that S-1 had bound to the fiber. Single fibers were solubilized in 25 μl of sample buffer immediately upon termination of an optical experiment, heated in boiling water, and stored at −20°C until needed. Silver staining followed the method of Morrisey (1981).

Electron microscopy

Fibers were fixed with 1% glutaraldehyde, 0.2% tannic acid in rigor buffer, postfixed with 1% O_5O_4, dehydrated in acetone, and embedded in plastic. Thin sections were mounted on copper grids, stained with saturated uranyl acetate, and counterstained with Reynold's lead citrate.

Theoretical model

Two new features have been incorporated into the theoretical analysis of the ellipsometry data (see Appendix, Chen et al., 1989). The first is a refinement step. Instead of computing the anisotropy of the myosin rod (form and intrinsic) as a whole, we split off the contributions of the LMM and that of S-2 separately. In this manner, S-2 orientations can be independently assigned in the overlapping and the nonoverlapping regions. The second feature incorporated in this analysis has to do with the introduction of exogenous S-1. The volume fraction of maximum S-1 addition was computed from estimating the number of sites available for its binding in a fiber stretched to its completely nonoverlapping condition (3.6 μm). This value is $f_{S\text{-}1\ add} = 0.058$. Our estimate of the maximum added S-1 was obtained in the following way. We know from earlier studies (Haskell et al., 1989) that the volume fraction of endogenous S-1 is ~0.023 in frog muscle. We know also that one thick filament contains 300 myosin molecules (600 S-1 heads) and that one thin filament contains ~380 actin molecules (Bagshaw, 1982). The thick-to-thin filament ratio (in each half-sarcomere) is 1:2. Thus, each thick filament would have four thin filaments or 1,520 actin monomers associated with it. Because 300 myosin molecules per thick filament represent a volume fraction of 0.023 then, assuming one S-1 head/actin monomer, a total exogenous S-1 volume fraction of 0.058 would be required to bind to all of the actin. In the case of zero overlap, this amount could be added to the fiber. In the case of full overlap, the situation is somewhat different because a portion of the endogenous S-1 is bound to actin in a rigor fiber. Using the estimate (Squire, 1981) that 67% of S-1 is bound in a full overlap, rigor fiber, we find that an additional (exogenous) S-1 volume fraction of 0.043 is possible leading to a total S-1 volume fraction of 0.066. In the case of a fiber at zero overlap, a total S-1 volume fraction (endogenous + exogenous) of 0.081 may be achieved. As the fiber is shortened, we have assumed a linear decrease in S-1 binding site availability in the I-band. In our model, the angle of tilt of S-1 in a fiber in the rigor state is a parameter that is variable. (This tilt angle is defined by the direction of the S-1 axis relative to the fiber axis.)

All the other parameters of our model were as discussed in Yeh and Baskin (1988) and Chen et al. (1989). Our volume fraction assignments were as follows:

F_{A_o}(A-band) = 0.040 including LMM S-2, and titin.
F_{s-1_o}(Endogenous S-1) = 0.023.
F_{I_o}(I-band) = 0.040 including F-actin, tropomyosin, troponin, Z-band material, and nebulin.

All "regions" were assumed to be optically isotropic, except for the A-band, which was assumed to be optically anisotropic. The angle of tilt of S-2 relative to the filament axis in the overlap region was set at 0°, while that in the nonoverlap region was assumed to be 20°.

RESULTS

S-1 purification was reliable and efficient. Fig. 1 *a* shows the SDS-PAGE of the preparation; S-1 was produced from the mhc of the myofibrils, retained during the rigor rinses after proteolysis, released into the supernatant with MgATP, and freed from almost all actin contamination by salting out at 37–70% ammonium sulfate (AS). A useful by-product of the procedure was the enriched actin in the 0–37% AS fraction; if actin was not removed by this step it proved extremely difficult to remove from the preparation. Fig. 1 *b* shows the gel pattern of the peak fractions of the anion-exchange chromatography. The S-1 containing peak fractions (24–41) were all virtually pure as determined by electrophoresis; the high salt purge eluted the contaminants (fraction 58–89) applied to the column with the S-1. The light chains 1 and 3 are not visible due to the low percentage (7.5%) of

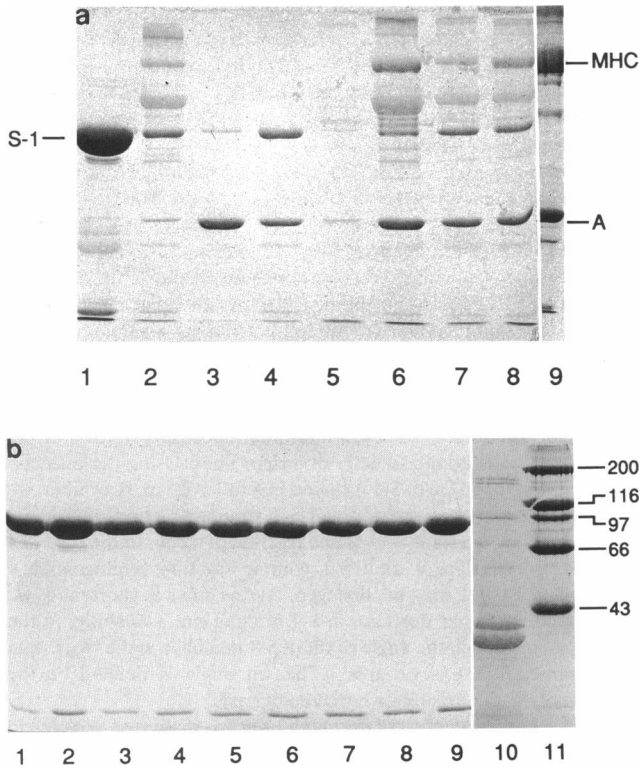

FIGURE 1 Electrophoresis of S-1 preparation steps from rabbit skeletal muscle myofibrils. (*a*) (lane *1*) Supernatant after centrifugation of low salt dialysis of ammonium sulfate-fractionated chymotryptic digest; (lane *2*) pellet after centrifugation of low salt dialysis of ammonium sulfate-fractionated chymotryptic digest; (lane *3*) pellet after centrifugation of 37% ammonium sulfate-treated chymotryptic digest in the presence of ATP; (lane *4*) supernatant after centrifugation of ATP-treated chymotryptic digest; (lane *5*) supernatant after centrifugation of chymotryptic digest before ATP-treatment; (lane *6*) pellet after centrifugation of ATP-treated chymotryptic digest; (lane *7*) 20-min chymotryptic digest; (lane *8*) 10-min chymotryptic digest; (lane *9*) total myofibrillar protein. (*b*) Electrophoretic analysis of peak fractions of S-1 preparation. Lanes *1–9* are samples from fractions 30–37 of the initial large peak; lane *10* is a sample of fraction 58 from trailing (high-salt-purge) peak; lane *11* are molecular weight markers. Numbers on the right represent molecular weight of standard proteins in kD.

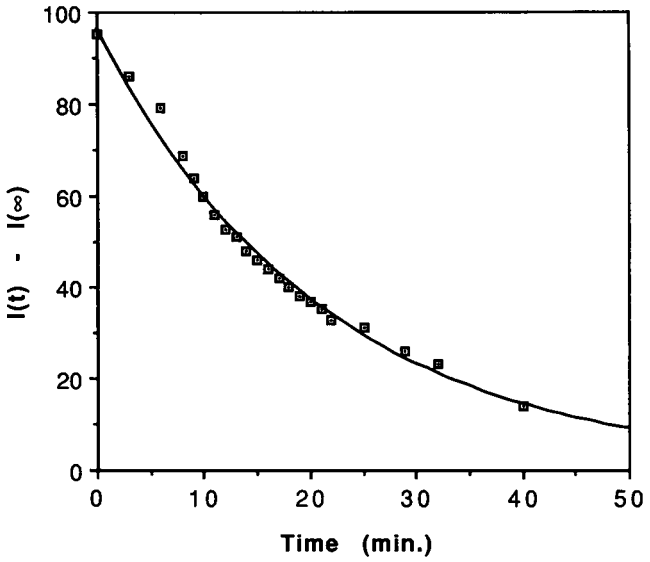

FIGURE 2 Plot of first order diffraction intensity versus time of incubation in 1 mg/ml S-1 of a single muscle fiber. Intensity decrease in time t is plotted as $I(t) - I(\infty)$ vs. time. The time constant of S-1 introduction is ~21 min assuming a single exponential decay ($r^2 = 0.992$). Sarcomere length was 3.0 μm.

gel used. S-1 preparations were enzymatically active with an average Ca ATPase activity of 0.60 ± 0.06 μmol P_i/mg S-1 per min. This value is similar to that reported by Thomas et al. (1980).

Incubation of the skinned single muscle fibers with the S-1 caused a decrease in the first diffraction order intensity due to the binding of the S-1 to the thin filaments and resulting decrease in the A/I band mass differential (the I-band mass was augmented by the S-1). Fig. 2 shows a typical curve of intensity as a function of time when a fiber was incubated in a solution containing 1 mg/ml S-1. The intensity showed a good fit to an exponential decay ($r^2 = 0.992$), indicating that a diffusion-limited first order reaction was occurring. The intensity could be returned to the original value by first rinsing away all S-1 not bound to actin and then releasing the S-1 with MgPPi. The ellipsometry parameters showed a similar reversibility and electrophoresis demonstrated the complete release of bound exo-S-1 by MgPPi (see below).

The change in the ellipsometry parameters and diffraction order intensity due to S-1 binding was progressive and could be reversed with MgPPi. Because it is our hypothesis that the source of our optical data is the binding of exo-S-1 to the thin filaments, the reversal of this process, i.e., the MgPPi release step, should also reverse, or return, the optical readings to or near the original. This was done (Fig. 3), and it was found that the optical signals did in fact respond in the expected fashion. The value of r_T increased due to binding of exo-S-1 to the fiber and decreased to close to the initial value when the fiber was treated with MgPPi and returned to the rigor condition, i.e., when exo-S-1 was released (see below). The response of the Δn_T signal to S-1 decoration of the same rigor fiber was consistent with our other experimental results (see below). It fell due to exo-S-1 binding and the MgPPi-release step reversed this reading. The diffraction order intensity

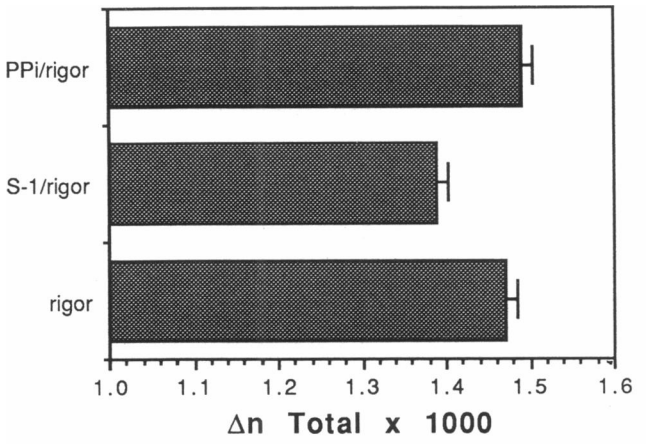

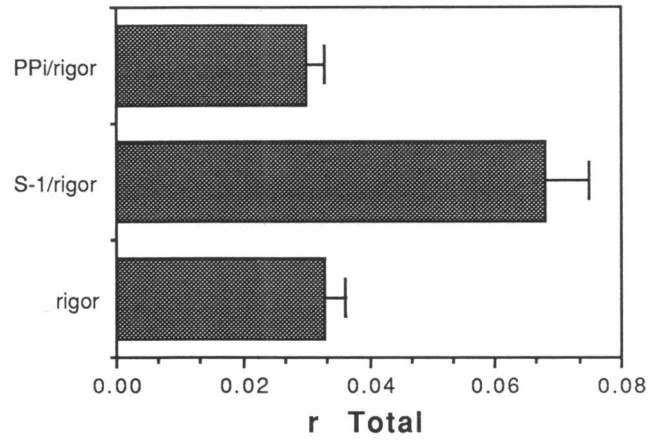

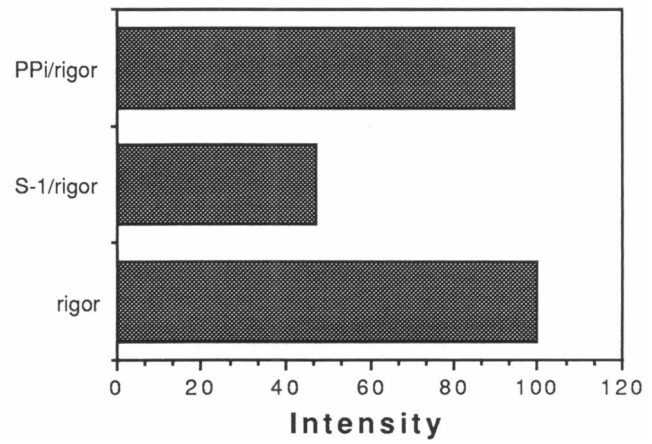

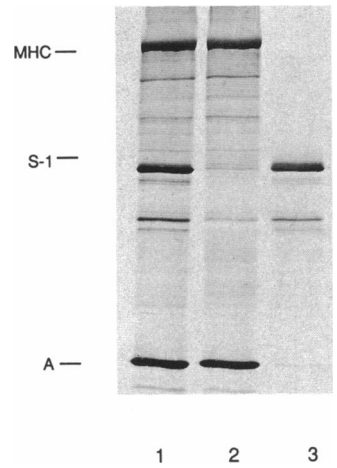

FIGURE 4 Electrophoresis of an S-1-treated fiber divided into halves that were then processed independently; one-half with PPi treatment and the other half without PPi treatment. (Lane *1*) Fiber-half of S-1-treated fiber not incubated with MgPPi before electrophoresis; (lane *2*) fiber-half of S-1-treated fiber incubated with MgPPi before electrophoresis; (lane *3*) MgPPi incubation medium from S-1-loaded fiber-half (from lane *2*).

showed similar responses to the experimental conditions (Fig. 3).

Electrophoresis in the presence of SDS under reducing conditions of single muscle fibers revealed the presence of a substantial amount of S-1 in the fiber (Fig. 4). Also shown is evidence that MgPPi releases bound exo-S-1 from the fiber. One single fiber was placed into rigor, incubated in S-1, rinsed with fresh rigor solution, and divided into halves. One-half was immediately processed for electrophoresis (Fig. 4, lane *1*) and the other half treated with MgPPi solution (Fig. 4, lane *2*). This half was then briefly rinsed in rigor solution and processed for electrophoresis, as was the MgPPI incubation solution (Fig. 4, lane *3*). This shows that exo-S-1 has bound to the fiber and can be released with PPi. The released S-1 was recoverable in the PPi incubation medium. It can be seen (lane *1*) that the quantity of bound S-1 is of the same order of magnitude as the quantity of myosin heavy chain, because the magnitude and intensity of the mhc band and the S-1 band are similar.

Electron microscopy (Fig. 5 *b*) localized the S-1 to the thin filaments. The appearance of the S-1-decorated thin filaments are similar to the 'arrowhead' structures initially viewed by Huxley (1963), and more recently by

FIGURE 3 Optical responses to S-1 incubation and MgPPi cycle of a single fiber. Sarcomere length was set at 3.3 μm. Fiber was placed into rigor, incubated with S-1, and then rinsed free of unbound S-1 with rigor buffer. The bound S-1 was released with a 5 mM MgPPi solution and returned to the rigor state. Differential field ratio error was ±0.007; birefringence error was ±2.5%.

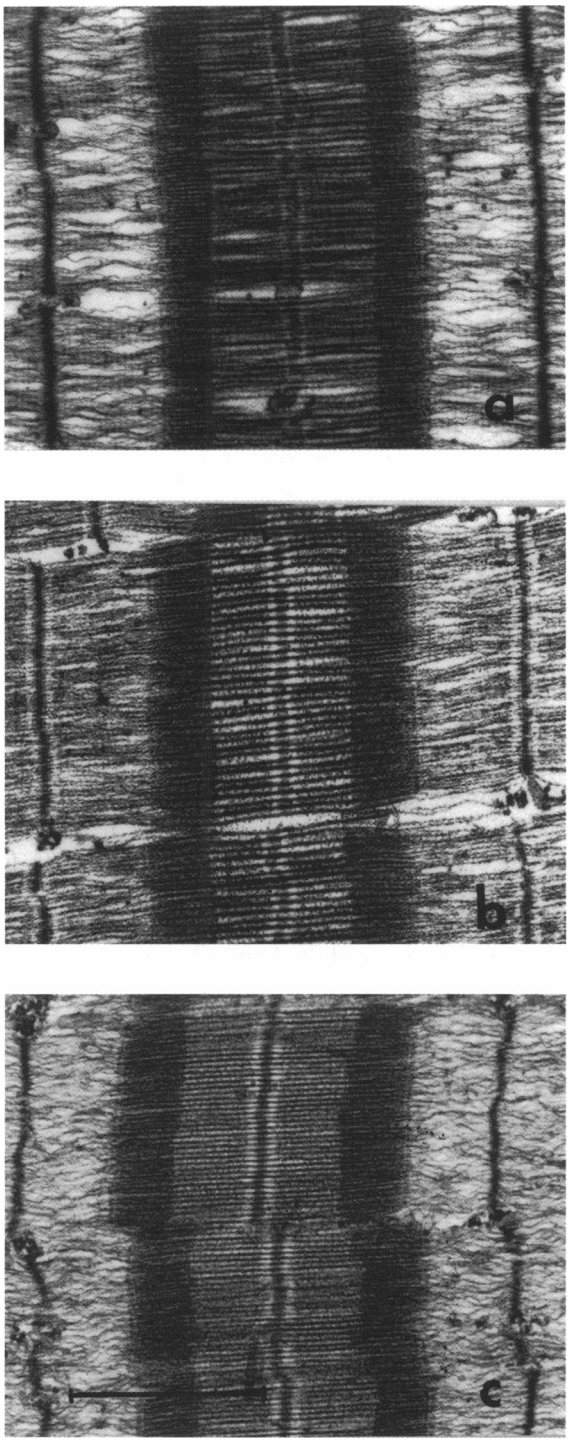

FIGURE 5 Electron micrographs of single muscle fibers fixed under the following conditions. (*a*) Control (untreated) fiber. (*b*) S-1-loaded fiber. (*c*) S-1-loaded fiber treated with MgPPi (sarcomere length in all cases was set at 3.0 μm).

Heuser and Cooke (1983). Due to the polarity of the thin filaments all of the S-1 molecules are oriented identically and decoration appears complete and uniform. Compared with the control (Fig. 5 *a*) the S-1-decorated thin filaments are straighter and more parallel. This could be due to an S-1-induced bundling effect on the thin filaments (Ando, 1987; Ando and Scales, 1985) and/or protection from the deleterious effects of certain fixatives on actin-containing filaments (Maupin-Szamier and Pollard, 1978). MgPPi appears to completely release S-1 from the thin filaments (Fig. 5 *c*), and Mg^{2+} as well as PPi was required for this action (data not shown).

Both the electron micrographs (Fig. 5) of fibers with bound S-1, and the gels of single fibers (Fig. 4), support our assumption of essentially total loading of actin sites with S-1 (an exogenous S-1 volume fraction of ~ 0.058 for a fiber at a sarcomere length of 3.6 μm). In binding studies using Tritium labeled S-1, Peckham and Irving (1989) concluded that their fibers were completely loaded and estimated that ~ 600 μM of bound S-1 was present in fibers with a sarcomere length of 3.69 μm after a 40 min incubation.

The optical data for all fibers are shown in Fig. 6. The results are grouped according to the sarcomere length of the fibers to the nearest tenth of a micron. The birefringence showed a small decrease at all sarcomere lengths. (Fiber diameter was measured in each fiber at each sarcomere length.)

Because each experiment involved measurements at only one sarcomere in length, and because optical measurements were made during only three different conditions of each fiber (rigor, rigor plus S-1, rigor after release of S-1), many different fibers were required. This introduced some variability into the results as is seen in the variance of the data (Fig. 6). Peckham and Irving (1989), using transmission birefringence to study similar preparations, reported an increase in birefringence, but the reported change was small ($\sim 5\%$). The sources of this discrepancy are addressed in the discussion.

The differential field ratio, r_T showed significant increases in all cases yet there appeared to be no simple sarcomere length dependency (Fig. 6 *b*). Longer sarcomere lengths would increase the I-band and so expose more thin filament S-1 binding sites. That is, there would be less competition from endogenous S-1 at longer sarcomere lengths and a greater amount of exogenous S-1 could bind.

DISCUSSION

This work, and indeed all birefringence studies, are sensitive to cross-bridge orientation in striated muscle

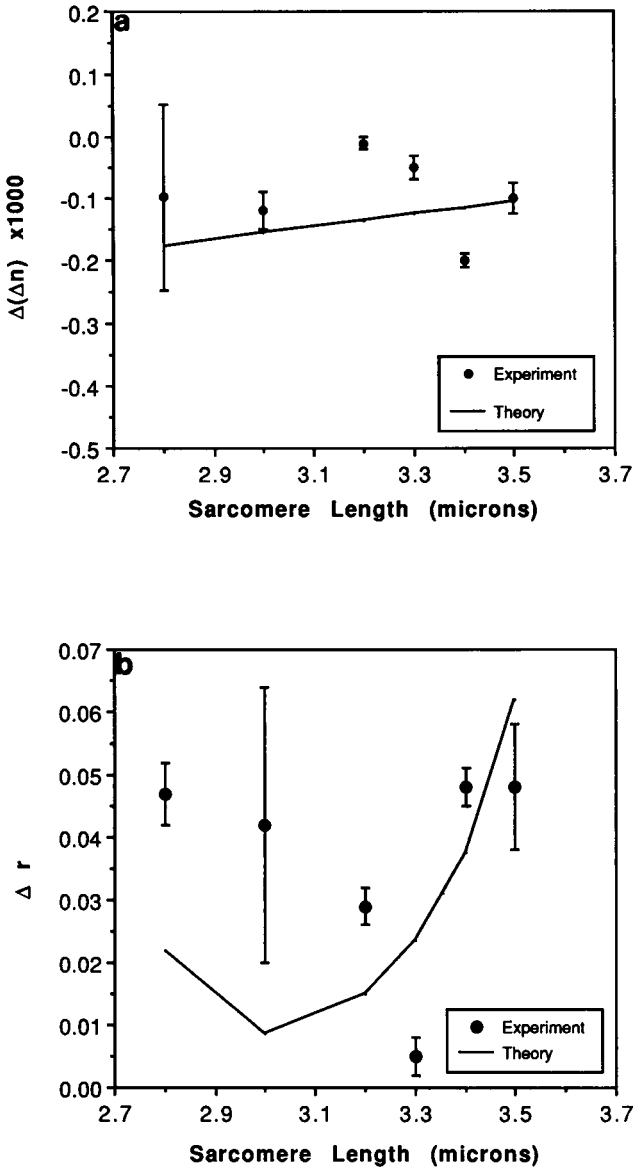

FIGURE 6 Summary of optical data. (*a*) Change in birefringence due to incubation in S-1. (*b*) Change in the differential field ratio. Error bars represent the standard deviation of the mean of the determinations for a given sarcomere length. Following are the sarcomere lengths in μm and the number of determinations in parentheses. 2.8 (2); 3.0 (2); 3.2 (1); 3.3 (3); 3.4 (1); 3.5 (5). Solid line represents theoretical data for S-1 binding angle of 68° and maximum exo-S-1 binding as described (see also Figs. 7 and 8).

and the results can be related to their function and behavior. This is done by modelling the source of the optical signal and it is this assignment that limits the technique's ability to discriminate among the possible explanations (cf. Haskell et al., 1989). This work uses optical ellipsometry to determine the contribution to the resultant optical polarization of a largely form S-1 element by measuring the signal change due to the binding of exogenous S-1 to the thin filaments of frog skeletal muscle. Based on the globular structure of S-1, with the helical regions folded (Vibert and Cohen, 1988), S-1 may be assumed to have little intrinsic anisotropy at the visible, 633-nm wavelength. In the types of experiments reported here, it is reasonable to consider its contribution to be almost exclusively of a form type. The total birefringence signal from skeletal muscle has both an intrinsic and a form component, corresponding to the molecular structure and the arrangement of the molecules, respectively, in a given medium. It is believed that the rod portion of the myosin heavy chain (mhc), due to the high α-helical content, influences intrinsic as well as form birefringence while the globular head region mostly effects form birefringence. The methods used here relied on reproducible alterations of the content of myosin subfragment S-1 *in situ,* namely the decoration of the thin filaments with S-1 and its release. Our attempts to investigate the contribution of exogenous HMM to the optical signal were thwarted by the poor penetration of this moiety into our skinned muscle fiber preparations. This would have allowed a direct comparison of strictly form enhancement (S-1) with the form-plus-intrinsic properties of HMM. HMM contains two heads plus a region of the rod, the S-2, which is thought to have some role in cross-bridge activity (Harrington, 1971; 1979; Huxley and Brown, 1967; Tsong et al., 1979) and could thus contribute to the change in optical anisotropy. This last point was in fact invoked by Taylor (1975) to explain his birefringence measurements on rabbit psoas muscle fibers during such conditions as relax-to-rigor transitions, pyrophosphate relaxation, etc. Because intrinsic birefringence seems to comprise a significant fraction of the total birefringence (Cassim et al., 1968; Colby, 1971; Fischer, 1947; Obiorah and Irving, 1989) and because the S-2 portion of the rod undergoes some orientational and/or conformational changes, it is plausible that part of the observed changes in birefringence during cross-bridge activity was due to the S-2. The specific electric birefringence ratio of HMM to S-1, determined by transient electric birefringence of these solutions (Highsmith and Eden, 1985), was ~35. This led the authors last cited to believe that "the birefringence (electric) of the HMM moiety would dominate the signal obtained from cross-bridge movement in skeletal muscle." This technique is, however, biased towards those elements with a permanent dipole, while our light scattering method observes those parts with an induced dipole. Also, as we discuss below, the angle of tilt of the heads alone can adequately explain our own findings.

As S-1 is added to a skinned muscle fiber the relative densities of the A and I regions of the sarcomere change.

Because the intensity of the diffraction lines is a function of the relative densities of the A and I bands, they will also change, leading at some volume fraction of added S-1 (~ 0.023), to a disappearance of the diffraction order line and, at larger volume fractions, to a reversal of the relative densities as the I region binds more S-1 and becomes more dense than the A region. Because, by definition, the differential field ratio (r_T) is inversely related to the diffraction intensity (its denominator is the sum of the parallel and perpendicular electric fields), it is dependent on the volume fraction of added S-1, as well as the S-1 binding angle.

The dependency of the change in the optical parameters Δn_T and r_T on S-1 binding to or its release from the thin filaments has been conclusively shown; they are sensitive indicators of exogenous S-1 binding. There are two important aspects to the decoration of the thin filaments with chymotryptic S-1. The increase in volume fraction of S-1 in discrete portions of the sarcomere and the axial binding angle of S-1 to the thin filaments can each have a major influence on birefringence and the differential field ratio (r_T).

The maximum volume fraction increase is sarcomere length-dependent due to competition from endogenous myosin heads for actin binding sites. Because there are 760 actin monomers for every 300 myosin heads in vertebrate muscle (Tregear and Squire, 1973) there are more than twice as many as endo-S-1. If, as discussed in Squire (1981), in a rigor fiber only 67% of the actin monomers in the overlap zone are labeled by an endo-S-1, then at full overlap 33% of the actin monomers could still bind exogenous-S-1. This would increase linearly to 100% at a sarcomere length of 3.6 μm where there is no overlap between thin and thick filaments and hence no binding of endo-S-1 to actin. Therefore, at full overlap nearly two times, and at nonoverlap 2.5 times, as many exogenous-S-1 could bind as the number of endo-S-1. Because the volume fraction of endo-S-1 in vertebrate-striated muscle is 0.023 (Bagshaw, 1982) this would mean an increase to 0.066 and 0.081, respectively, in the volume fraction of S-1. These approximations were used to calculate the change in Δn_T according to the theory of Yeh and Baskin (1988). The values for Δn_T were derived for the added volume fractions of 0.043 and 0.058 for a sarcomere length range of 2.2 to 3.6 μm.

We next developed a modified version of our theory (Yeh and Baskin, 1988) that dealt with the incorporation of S-1 into the fiber (see Theoretical model section). We modelled this incorporation at different assumed axial binding angles of S-1 to actin and compared the values of Δn_T and r_T that resulted (Fig. 7, *a* and *b*) with the experimentally determined values. The experimentally determined change in Δn_T with change in sarcomere length was small, and small (but significant) changes

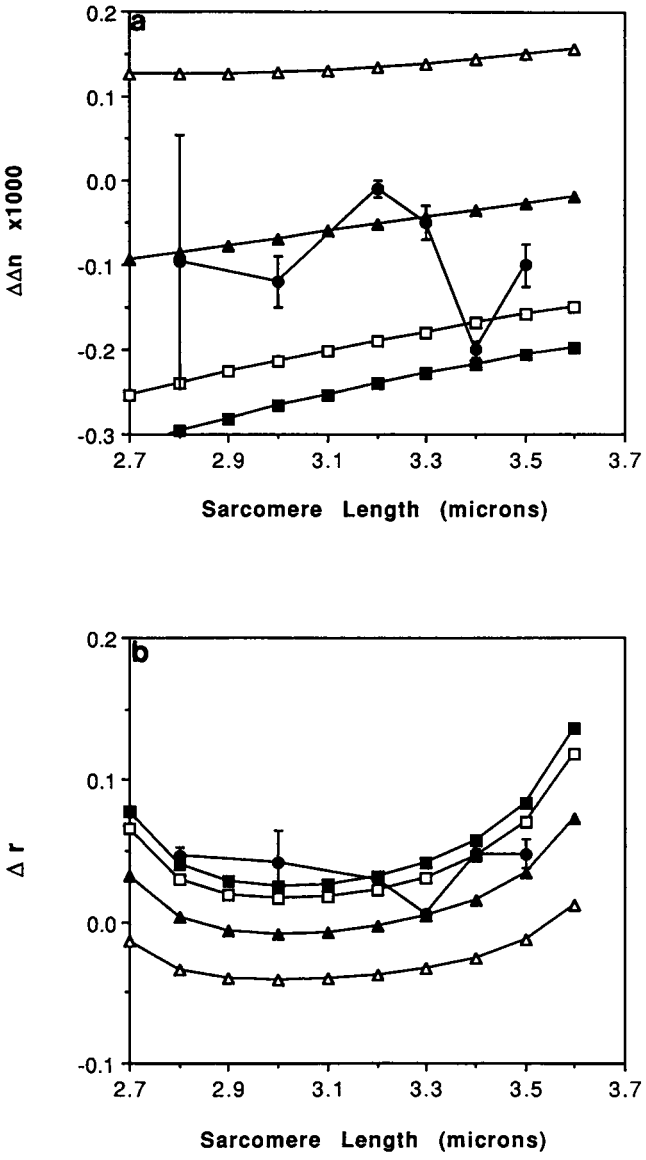

FIGURE 7 Plots of model simulations in which the angle of S-1 attachment to actin was varied for all S-1. Fig. 7, *a* and *b* show the response of birefringence and r_T to the angle of S-1 binding to the thin filaments calculated for 67% endogenous S-1 bound to actin. Plot symbols are: measured values (●); 45° (△); 60° (▲); 75° (□); 90° (■).

were seen in the values of Δn_T modelled for different average angles of attachment of S-1. In contrast, r_T shows large changes upon S-1 addition and the theoretical values are strongly dependent on attachment angle of S-1 to actin. We found, however, that changes in this angle produced changes in Δn_T that exceeded those produced by volume fraction increases. Fig. 7, *a* and *b* shows the results obtained for S-1 binding angles of 45, 60, 75, and 90 degrees. The volume fraction increase due

to exo-S-1 binding ranged between 0.043 at SL = 2.8 μm to 0.058 at SL = 3.6 μm.

The experimental results tend to support an average S-1 to actin, rigor binding angle in the 60° to 75° range. The values of $\Delta(\Delta n_T)$ (change in birefringence upon S-1 addition), which were experimentally determined, overlap the theoretical curve for 60° and 75° (see Fig. 7 *a*) and 68° is a mean value. Lower value of S-1 binding angle (45°) and higher binding angle (90°) show no overlap between $\Delta(\Delta n_T)_{\text{Theoretical}}$ and $\Delta(\Delta n_T)_{\text{Measured}}$.

In the case of Δr_T (the change in the differential field ratio caused by addition of S-1), the fit to the data is better at an attachment angle of 60°–75° than at any lesser angle (Fig. 7 *b*). Taken together, the experimental results support an average S-1 binding angle (rigor) of 68° ± 7°. Due to the variability in our data (Fig. 6) we are not able to make a more precise determination of the S-1 angle. At this stage of our work we are only claiming a qualitative relationship between theory and experiment. The fact that the theory is of the correct order of magnitude and correctly predicts the trend of the data is our major accomplishment.

In early studies, addition of ATP to rigor muscle caused a structural change; both electron microscopy and x-ray diffraction suggest that myosin projections are tilted in rigor but perpendicular in relaxed muscle (Wray and Holmes, 1981). The results of a number of studies appear to show that the angle of tilt is ~45° (see Craig et al., [1985] for references). In a recent study, Peckham and Irving (1989) concluded, based on birefringence studies and a cross-bridge model, that the angle of S-1 attachment to actin in a rigor fiber was ~50°. Thus, our conclusion that the mean axial angle of myosin heads (both native and added) is larger, with a value of 68° ± 7°, is at variance with these studies. Taylor and Amos (1981), however, in studies of the binding of myosin cross-bridges to thin filaments, indicate that an axial binding angle of S-1 to the thin filament of 55° to 65° is consistent with their data and with the data of Wakabayashi and Toyoshima (1981).

It is important to emphasize that modification of our theoretical model to fit the smaller axial angle would require changes in the values of volume fraction of components and/or refractive index of regions of the sarcomere. Because our model (Yeh and Baskin, 1988) has been quite successful in fitting data from skinned and intact fiber experiments (Chen et al., 1989), as well as in studies using insect fibers (Baskin et al., 1989), we have no independent basis for making such modifications.

It is also possible that the added S-1 attaches at a different axial angle than the native S-1. In Fig. 8 we show the change in birefringence (ΔΔn) for the situation where endogenous S-1 is at an angle of 68° to the fiber

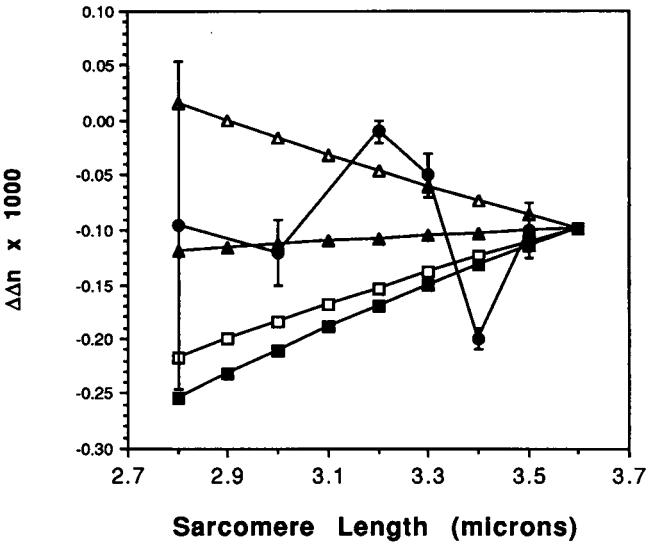

FIGURE 8 Experimental data (●) of the change in birefringence, ΔΔn, superimposed on the theoretical plots of the corresponding quantities for the purpose of modelling the tilt angle of the exogenously-introduced S-1. The curves showing different tilt angle, 45° (△), 60° (▲), 75° (□), and 90° (■), apply only to those S-1 exogenously added; the endogenous S-1 have been assumed to maintain the averaged rigor tilt angle of 68°.

axis and exogenous S-1 assumes different angles. Again, at an exogenous S-1 angle of 60°, the fit to the birefringence data is best.

Even allowing for variance in our measurements of birefringence and differential field ratio, we still find a larger average axial angle (60°–75°) for all exogenous and endogenous S-1 in a rigor fiber fits our data better than the smaller (45°–50°) angle usually attributed to S-1 in a rigor muscle (Reedy et al., 1965). It is also important to note that our model fits data that shows both a negative value of birefringence change $\Delta(\Delta n_T)$ and a positive value of differential field ratio change Δr_T.

In most studies of cross-bridge structure in rigor muscle, the assumption has been made that all the bound cross-bridges are in exactly the same orientation with the same axial angle of attachment of S-1 to actin. This axial angle is usually found to be between 45° and 50° in agreement with early electron micrographs of Reedy et al. (1965). In recent studies, however (Taylor et al., 1989), evidence for two rigor cross-bridge orientations was found in insect muscle. "Dense" appearing lead bridges angled at ~45° contrasted with "less dense" rear bridges angled at ~90° to the filament axis. The dense lead bridges were found to be in the majority, however, the number of rear bridges was not trivial. It appears likely that in such a fiber, birefringence and DFR studies would lead to an estimated axial angle

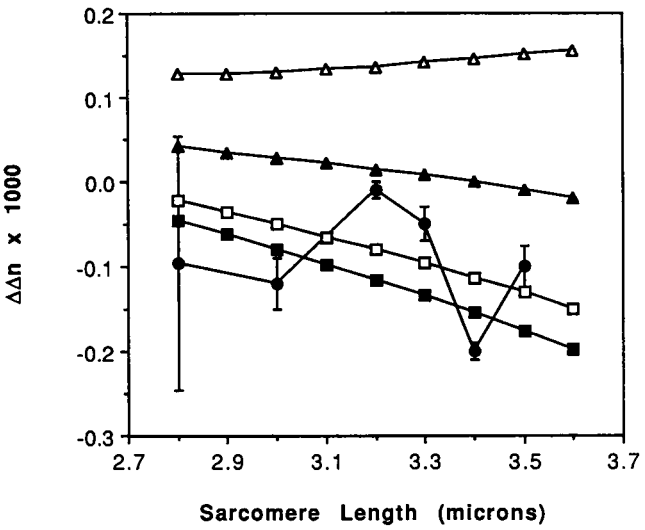

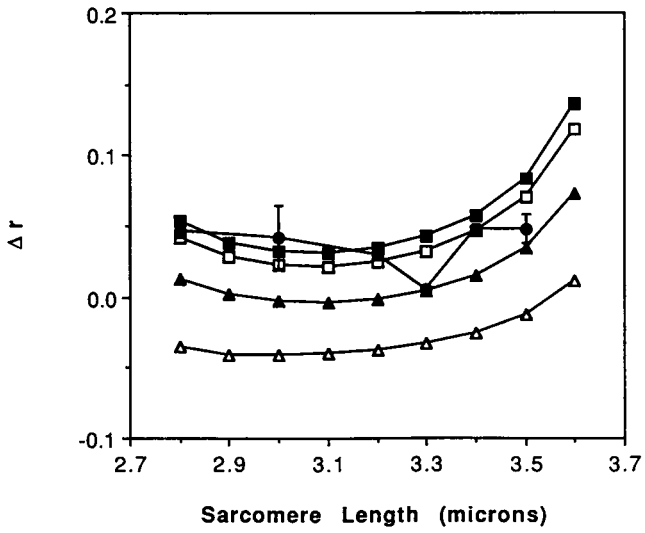

FIGURE 9 Plots of model simulations in which the angle of S-1 attachment to actin (for all S-1) was varied. In this case it was assumed that 100% of the endogenous S-1 is bound to actin. Experimental values (●); 45° (△); 60° (▲); 75° (□); 90° (■).

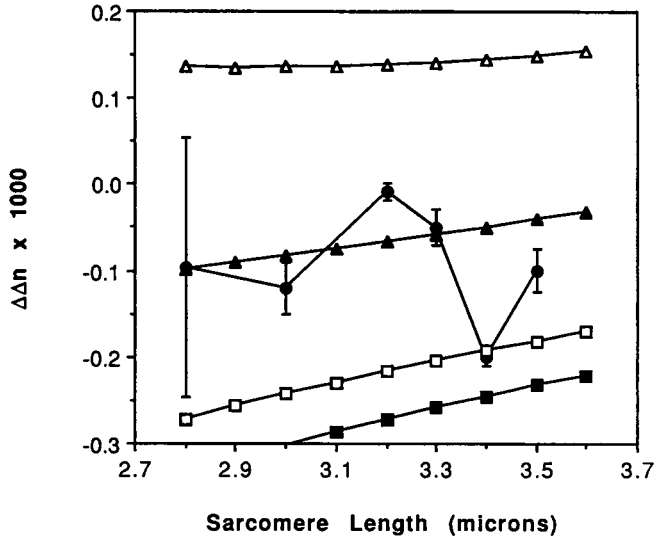

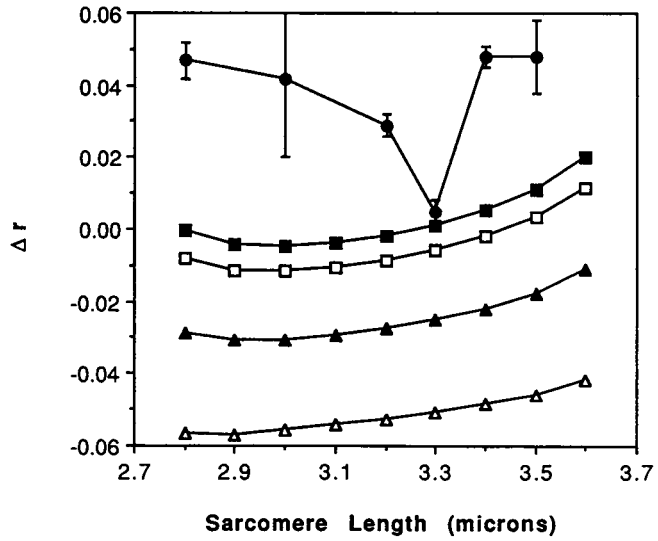

FIGURE 10 Plots of model simulation calculated assuming a ratio of actin monomers to endogenous S-1 of 3.25 (all previous data assumed a ratio of 2.53). Plots are for different angles of all S-1 attachment to actin. Experimental values (●); 45° (△); 60° (▲); 75° (□); 90° (■).

greater than 45°–50° because it would represent a weighted average of lead and rear cross-bridges. Thus, our estimate of an axial S-1 angle in rigor frog fibers (60°–75°) may represent a weighted average of two or more angles.

It is also possible that our estimate of an average S-1 axial angle of 68° ± 7° represents an average of different endogenous and exogenous S-1 angles. There is no direct evidence on this point because the precise measurements of Reedy et al. (1990) have not been done on skinned frog fibers with added (exogenous) S-1.

In all of our calculations we have assumed that 67% of the endogenous S-1 in the overlap region binds to actin. In Fig. 9 we show the fit to the experimental data when we assume 100% of the endogenous S-1 in the overlap region binds to actin. While the DFR shows only a small change, the change in birefringence, ($\Delta(\Delta n)$), shows a better fit at an S-1 angle of ~75°. Intermediate values of

the percentage of bound endogenous S-1 would therefore support the higher value of S-1 angle (i.e., 68°).

We have also, in previous calculations, assumed a ratio of 2.53 actin monomers to endogenous S-1. Other workers (Yates and Greaser, 1983), however, have estimated this ratio at 3.25. In Fig. 10 we show the results of using a ratio of 3.25 acting monomers to one endogenous S-1 molecule in our model. In this case, the fit to the birefringence data is only very slightly altered but the fit to the change in DFR data becomes very poor showing no overlap at any of the calculated S-1 angles.

Because our data is an average of all cross-bridges we are unable to accurately describe the range of cross-bridge orientations, i.e., an average angle may be produced by a narrow or broad range. The use of a probe sensitive to the dynamics of cross-bridge orientation, photon correlation spectroscopy, is currently being developed (Yeh et al., 1990) in order to provide more detailed information concerning the range of angles occupied by cross-bridges under experimental conditions.

Received for publication 15 October 1990 and in final form 16 July 1991.

REFERENCES

Ando, T. 1987. Bundling of myosin sub-fragment 1 decorated actin filaments. *J. Mol. Biol.* 195:351–358.

Ando, T., and D. Scales. 1985. Skeletal muscle myosin sub-fragment 1 induces bundle formation by actin filaments. *J. Biol. Chem.* 260:2321–2327.

Bagshaw, C. 1982. *In* Outline Studies in Biology. *Muscle Contraction.* Chapman and Hall, New York, NY. 60–66.

Baskin, R., Y. Yeh, K. Burton, J. Chen, and M. Jones. 1986. Optical depolarization changes in single skinned muscle fibers. *Biophys. J.* 50:63–74.

Baskin, R. J., S. Shen, and Y. Yeh. 1989. Optical measurements on isolated single fibers from insect flight muscle. *J. Physiol.* 418:55P.

Brenner, B., L. C. Yu, and R. J. Podolsky. 1984. X-ray diffraction evidence for cross-bridge formation in relaxed muscle fibers at various ionic strengths. *Biophys. J.* 46:299–306.

Cassim, J., P. Tobias, and E. Taylor. 1968. Birefringence of muscle proteins and the problem of structural birefringence. *Biochim. Biophys. Acta.* 168:463–471.

Chen, J. S., R. J. Baskin, R. James Baskin, K. Burton, S. Shen, and Y. Yeh. 1989. Polarization states of diffracted light: changes accompanying fiber activation. *Biophys. J.* 56:595–605.

Colby, R. 1971. Intrinsic birefringence of glycerinated myofibrils. *J. Cell Biol.* 51:763–771.

Craig, R., L. E. Greene, and E. Eisenberg. 1985. Structure of the actin-myosin complex in the presence of ATP. *Proc. Natl. Acad. Sci. USA.* 82:3247–3251.

Fischer, E. 1947. Birefringence and ultrastructure of muscle. *Ann. NY Acad. Sci.* 47:783–795.

Harrington, W. 1971. A mechanochemical mechanism for muscle contraction. *Proc. Natl. Acad. Sci. USA.* 68:685–689.

Harrington, W. 1979. On the origin of contractile force in skeletal muscle. *Proc. Natl. Acad. Sci. USA.* 76:5066–5070.

Haskell, R. C., F. D. Carlson, and P. S. Blank. 1989. Form birefringence of muscle. *Biophys. J.* 56:401–413.

Heuser, J., and R. Cooke. 1983. Actin-myosin interaction visualized in freeze-etch, deep-etch replica technique. *J. Mol. Biol.* 169:97–122.

Highsmith, S., and D. Eden. 1985. Transient electric birefringence characterization of heavy meromyosin. *Biochemistry.* 24:4917–4924.

Huxley, H. E. 1963. Electron microscope studies on the structure of natural and synthetic protein filaments from striated muscle. *J. Mol. Biol.* 1:281–308.

Huxley, H. E., and W. Brown. 1967. The low angle x-ray diagram of vertebrate striated muscle and its behavior during contraction and rigor. *J. Mol. Biol.* 104:747–775.

Irving, M., and M. Peckham. 1986. Birefringence as a probe of crossbridge orientation in demembranated muscle fibers of frog and rabbit. *J. Physiol.* 377:95P.

Laemmli, U. K. 1970. Cleavage of structural proteins during the assembly of the head of bacteriophages T4. *Nature (Lond.).* 227:680–685.

Magid, A., and M. K. Reedy. 1980. X-ray diffraction observations of chemically skinned frog skeletal muscle processed by an improved method. *Biophys. J.* 30:27–40.

Margossian, S., and S. Lowey. 1982. Preparation of myosin and its sub-fragments from rabbit skeletal muscle. *Methods Enzymol.* 85:55–71.

Matsubara, I., and G. F. Elliot. 1972. X-ray diffraction studies on skinned single fibers of frog skeletal muscle. *J. Mol. Biol.* 72:657–669.

Maupin-Szamier, P., and T. Pollard. 1978. Actin filament destruction by osmium tetroxide. *J. Cell Biol.* 77:837–852.

Morrisey, J. 1981. Silver strain for proteins in polyacrylamide gels: a modified procedure with enhanced uniform sensitivity. *Anal. Biochem.* 117:307–310.

Obiorah, O., and M. Irving. 1989. The intrinsic birefringence of skinned muscle fibers in aqueous and non-aqueous media. *Biophys. J.* 55:462*a*. (Abstr.)

Peckham, M., and M. Irving. 1989. Myosin crossbridge orientation in demembranated muscle fibers studied by birefringence and x-ray diffraction measurements. *J. Mol. Biol.* 210:113–126.

Reedy, M. K., K. C. Holmes, and R. T. Tregear. 1965. Induced changes in orientation of the crossbridges of glycerinated insect flight muscle. *Nature (Lond.).* 207:1276–1280.

Squire, J. 1981. The Structural Basis of Muscular Contraction. Plenum Publishing Corp., New York. 106–130.

Taylor, D. 1975. Birefringence changes in vertebrate striated muscle. *J. Supramol. Struct.* 3:181–191.

Taylor, D. 1976. Quantitative studies on the polarization optical properties of striated muscle. I. Birefringence changes of rabbit psoas muscle in the transition from rigor to relaxed state. *J. Cell Biol.* 68:497–511.

Taylor, K., and L. Amos. 1981. A new model for the geometry of the binding of myosin crossbridges to muscle thin filaments. *J. Mol. Biol.* 147:297–324.

Taylor, K. A., M. C. Reedy, L. Cordova, and M. K. Reedy. 1989. Three-dimensional image reconstruction of insect flight muscle. I. The rigor myac layer. *J. Cell Biol.* 109:1085–1102.

Thomas, D., S. Ishiwata, J. Seidel, and J. Gergely. 1980. Submillisecond rotational dynamics of spin-labeled myosin heads in myofibrils. *Biophys. J.* 32:873–890.

Tregear, R., and J. Squire. 1973. Myosin content and filament structure in smooth and striated muscle. *J. Mol. Biol.* 77:279–290.

Tsong, T., T. Karr, and W. Harrington. 1979. Rapid helix-coil transitions in the S-2 region of myosin. *Proc. Natl. Acad. Sci. USA.* 76:1109–1113.

Ueno, H., and W. Harrington. 1986. Local melting in the subfragment-2 region of myosin in activated muscle and its correlation to contractile force. *J. Mol. Biol.* 190:69–82.

Vibert, P., and C. Cohen. 1988. Domains, motions and regulation in the myosin head. *J. Muscle Res. Cell Motil.* 9:296–305.

Wakabayashi, T., and C. Toyoshima. 1981. Three-dimensional image analysis of the complex of thin filaments and myosin molecules from skeletal muscle. II. The multi-domain structure of actin-myosin complex. *J. Biochem. (Tokyo).* 90:683–701.

Wray, J. S., and K. C. Holmes. 1981. X-ray diffraction studies of muscle. *Annu. Rev. Physiol.* 43:553–565.

Yates, L. D., and M. L. Greaser. 1983. Quantitative determination of myosin and actin in rabbit skeletal muscle. *J. Mol. Biol.* 168:123–141.

Yeh, Y., and R. Baskin. 1988. Theory of optical ellipsometric measurements from muscle diffraction studies. *Biophys. J.* 54:205–218.

Yeh, Y., R. Baskin, S. Shen, and M. Jones. 1990. Photon correlation spectroscopy of the polarization signal from signal muscle fibers. *J. Muscle Res. Cell Motil.* 11:137–146.